

# $Q^2$ Evolution of the Neutron Spin Structure Moments using a $^3\text{He}$ Target.

M. Amarian,<sup>24</sup> L. Auerbach,<sup>20</sup> T. Averett,<sup>6,23</sup> J. Berthot,<sup>4</sup> P. Bertin,<sup>4</sup> B. Bertozzi,<sup>11</sup> T. Black,<sup>11</sup> E. Brash,<sup>16</sup> D. Brown,<sup>10</sup> E. Burtin,<sup>18</sup> J. Calarco,<sup>13</sup> G. Cates,<sup>15,22</sup> Z. Chai,<sup>11</sup> J.-P. Chen,<sup>6</sup> Seonho Choi,<sup>20</sup> E. Chudakov,<sup>6</sup> E. Cisbani,<sup>5</sup> C.W. de Jager,<sup>6</sup> A. Deur,<sup>4,6,22</sup> R. DiSalvo,<sup>4</sup> S. Dieterich,<sup>17</sup> P. Djawotho,<sup>23</sup> M. Finn,<sup>23</sup> K. Fissum,<sup>11</sup> H. Fonvieille,<sup>4</sup> S. Frullani,<sup>5</sup> H. Gao,<sup>11</sup> J. Gao,<sup>1</sup> F. Garibaldi,<sup>5</sup> A. Gasparian,<sup>3</sup> S. Gilad,<sup>11</sup> R. Gilman,<sup>6,17</sup> A. Glamazdin,<sup>9</sup> C. Glashauser,<sup>17</sup> E. Goldberg,<sup>1</sup> J. Gomez,<sup>6</sup> V. Gorbenko,<sup>9</sup> J.-O. Hansen,<sup>6</sup> B. Hersman,<sup>13</sup> R. Holmes,<sup>19</sup> G.M. Huber,<sup>16</sup> E. Hughes,<sup>1</sup> B. Humensky,<sup>15</sup> S. Incerti,<sup>20</sup> M. Iodice,<sup>5</sup> S. Jensen,<sup>1</sup> X. Jiang,<sup>17</sup> C. Jones,<sup>1</sup> G. Jones,<sup>8</sup> M. Jones,<sup>23</sup> C. Jutier,<sup>4,14</sup> A. Ketikyan,<sup>24</sup> I. Kominis,<sup>15</sup> W. Korsch,<sup>8</sup> K. Kramer,<sup>23</sup> K. Kumar,<sup>12,15</sup> G. Kumbartzki,<sup>17</sup> M. Kuss,<sup>6</sup> E. Lakuriqi,<sup>20</sup> G. Laveissiere,<sup>4</sup> J. Leroise,<sup>6</sup> M. Liang,<sup>6</sup> N. Liyanage,<sup>6,11</sup> G. Lolos,<sup>16</sup> S. Malov,<sup>17</sup> J. Marroncle,<sup>18</sup> K. McCormick,<sup>14</sup> R. Mckeown,<sup>1</sup> Z.-E. Meziari,<sup>20</sup> R. Michaels,<sup>6</sup> J. Mitchell,<sup>6</sup> Z. Papandreou,<sup>16</sup> T. Pavlin,<sup>1</sup> G.G. Petratos,<sup>7</sup> D. Pripstein,<sup>1</sup> D. Prout,<sup>7</sup> R. Ransome,<sup>17</sup> Y. Roblin,<sup>4</sup> D. Rowntree,<sup>11</sup> M. Rvachev,<sup>11</sup> F. Sabatie,<sup>14</sup> A. Saha,<sup>6</sup> K. Slifer,<sup>20</sup> P. Souder,<sup>19</sup> T. Saito,<sup>21</sup> S. Strauch,<sup>17</sup> R. Suleiman,<sup>7</sup> K. Takahashi,<sup>21</sup> S. Tejiro,<sup>21</sup> L. Todor,<sup>14</sup> H. Tsubota,<sup>21</sup> H. Ueno,<sup>21</sup> G. Urciuoli,<sup>5</sup> R. Van der Meer,<sup>6,16</sup> P. Vernin,<sup>18</sup> H. Voskanian,<sup>24</sup> B. Wojtsekhowski,<sup>6</sup> F. Xiong,<sup>11</sup> W. Xu,<sup>11</sup> J.-C. Yang,<sup>2</sup> B. Zhang,<sup>11</sup> P. Zolnierczuk<sup>8</sup>

(Jefferson Lab E94010 Collaboration)

<sup>1</sup>California Institute of Technology, Pasadena, California 91125

<sup>2</sup>Chungnam National University, Taejeon 305-764, Korea

<sup>3</sup>Hampton University, Hampton, Virginia 23668

<sup>4</sup>LPC IN2P3/CNRS, Université Blaise Pascal, F-63170 Aubière Cedex, France

<sup>5</sup>Istituto Nazionale di Fisica Nucleare, Sezione Sanità, 00161 Roma, Italy

<sup>6</sup>Thomas Jefferson National Accelerator Facility, Newport News, Virginia 23606

<sup>7</sup>Kent State University, Kent, Ohio 44242

<sup>8</sup>University of Kentucky, Lexington, Kentucky 40506

<sup>9</sup>Kharkov Institute of Physics and Technology, Kharkov 310108, Ukraine

<sup>10</sup>University of Maryland, College Park, Maryland 20742

<sup>11</sup>Massachusetts Institute of Technology, Cambridge, Massachusetts 02139

<sup>12</sup>University of Massachusetts-Amherst, Amherst, Massachusetts 01003

<sup>13</sup>University of New Hampshire, Durham, New Hampshire 03824

<sup>14</sup>Old Dominion University, Norfolk, Virginia 23529

<sup>15</sup>Princeton University, Princeton, New Jersey 08544

<sup>16</sup>University of Regina, Regina, SK S4S 0A2, Canada

<sup>17</sup>Rutgers, The State University of New Jersey, Piscataway, New Jersey 08855

<sup>18</sup>CEA Saclay, DAPNIA/SPHN, F-91191 Gif/Yvette, France

<sup>19</sup>Syracuse University, Syracuse, New York 13244

<sup>20</sup>Temple University, Philadelphia, Pennsylvania 19122

<sup>21</sup>Tohoku University, Sendai 980, Japan

<sup>22</sup>University of Virginia, Charlottesville, Virginia 22904

<sup>23</sup>The College of William and Mary, Williamsburg, Virginia 23187

<sup>24</sup>Yerevan Physics Institute, Yerevan 375036, Armenia

(Dated: October 25, 2018)

We have measured the spin structure functions  $g_1$  and  $g_2$  of  $^3\text{He}$  in a double-spin experiment by inclusively scattering polarized electrons at energies ranging from 0.862 to 5.058 GeV off a polarized  $^3\text{He}$  target at a  $15.5^\circ$  scattering angle. Excitation energies covered the resonance and the onset of the deep inelastic regions. We have determined for the first time the  $Q^2$  evolution of  $\Gamma_1(Q^2) = \int_0^1 g_1(x, Q^2) dx$ ,  $\Gamma_2(Q^2) = \int_0^1 g_2(x, Q^2) dx$  and  $d_2(Q^2) = \int_0^1 x^2 [2g_1(x, Q^2) + 3g_2(x, Q^2)] dx$  for the neutron in the range  $0.1 \text{ GeV}^2 \leq Q^2 \leq 0.9 \text{ GeV}^2$  with good precision.  $\Gamma_1(Q^2)$  displays a smooth variation from high to low  $Q^2$ . The Burkhardt-Cottingham sum rule holds within uncertainties and  $d_2$  is non-zero over the measured range.

PACS numbers: 25.30.-c, 11.55.Hx, 11.55.Fv, 12.38.Qk

During the past twenty five years, our understanding of Quantum Chromodynamics (QCD) has advanced through the study of the spin structure of the nucleon. Measurements of the nucleon spin structure functions  $g_1$  and  $g_2$  in deep inelastic lepton scattering (DIS) were used

to unravel the spin structure of the nucleon in terms of its constituents, quarks and gluons, and test QCD. Among the important results are the finding that only a small fraction (about 20%) of the nucleon spin is accounted for by the spin of quarks [1], and the test of the Bjorken sum

rule [2], a fundamental sum rule of QCD, to better than 10%. To make this latter test possible and determine the quark contribution to the total spin, it was essential to calculate the corrections necessary to evolve the Bjorken sum rule and the first moment of  $g_1$  [3] to  $Q^2$  values accessible experimentally. To this end the sum rule, originally derived in the limit  $Q^2 \rightarrow \infty$  using current algebra, was generalized using the technique of operator product expansion (OPE) in QCD [4, 5, 6, 7]. In this connection, it was also realized that the Bjorken sum rule was a special case of a more general sum rule known as the extended Gerasimov-Drell-Hearn (GDH) sum rule [8] which spans the full range of momentum transfer from  $Q^2 = 0$  to  $Q^2 \rightarrow \infty$ .

At small  $Q^2$ , after subtracting the elastic contribution,  $\bar{\Gamma}_1(Q^2) = \Gamma_1(Q^2) - \Gamma_1(Q^2)^{\text{elastic}}$ , is linked to the anomalous magnetic moment of the nucleon  $\kappa$  by

$$\bar{\Gamma}_1(Q^2) = \int_0^{x_0} g_1(x, Q^2) dx = -\frac{Q^2}{8M^2} \kappa^2 + O\left(\frac{Q^4}{M^4}\right), \quad (1)$$

where  $x_0$  coincides with the nucleon pion threshold. The first term in the right hand side of (1) corresponds to the original GDH sum rule prediction [9]. The next term has been evaluated by Ji *et al.* using a heavy-baryon chiral perturbation theory (HB $\chi$ PT) [8, 10] and by Bernard *et al.* using a covariant chiral perturbation theory ( $\chi$ PT) [11, 12].

At large  $Q^2$  ( $Q^2 \gg \Lambda_{QCD}^2$ )  $\Gamma_1(Q^2)$  is expressed in terms of a twist expansion [13, 14]:

$$\Gamma_1(Q^2) = \frac{1}{2} a_0 + \frac{M^2}{9Q^2} (a_2 + 4d_2 + 4f_2) + O\left(\frac{M^4}{Q^4}\right), \quad (2)$$

where  $a_0$  is the dominant, leading twist contribution. It is determined, apart from QCD radiative corrections [6], by the triplet  $g_A$  and octet  $a_8$  axial charges and the net quark spin contribution to the total nucleon spin. These axial charges are extracted from measurements of the neutron and hyperons weak decay measurements [15]. Here  $a_2$  is a second moment of the  $g_1$  structure function and arises from the target mass correction [14]. The quantities  $d_2$  and  $f_2$  are the twist-3 and the twist-4 reduced matrix elements. These matrix elements contain non-trivial quark-gluon interactions beyond the parton model. A first attempt at extracting  $f_2$  has been carried out by Ji and Melnitchouk [16] using the world data but with poor statistics below  $Q^2 = 1 \text{ GeV}^2$ . In QCD,  $d_2$  and  $f_2$  can be expressed as linear combinations of the induced color electric and magnetic polarizabilities  $\chi_E$  and  $\chi_B$  [17, 18] when a nucleon is polarized. The above twist expansion may be valid down to  $Q^2 = 0.5 \text{ GeV}^2$  if higher order terms are small.

We define  $d_2$  as the second moment of a particular combination of the measured  $g_1$  and  $g_2$  structure func-

tions:

$$\begin{aligned} d_2(Q^2) &= \int_0^1 x^2 [2g_1(x, Q^2) + 3g_2(x, Q^2)] dx \quad (3) \\ &= 3 \int_0^1 x^2 [g_2(x, Q^2) - g_2^{WW}(x, Q^2)] dx \end{aligned}$$

where  $g_2^{WW}$ , known as the Wandzura-Wilczek [22] term, depends only on  $g_1$

$$g_2^{WW}(x, Q^2) = -g_1(x, Q^2) + \int_x^1 \frac{g_1(y, Q^2)}{y} dy. \quad (4)$$

The quantity  $d_2$  reduces to a twist-3 matrix element at large  $Q^2$  where an OPE expansion becomes valid.

The advantages of measuring higher moments of the spin structure functions are twofold; 1) the kinematical region experimentally accessible gives most of the contribution to these moments, and 2) the matrix elements in the OPE of these moments can be calculated using lattice QCD [19].

Most of the previous measurements of  $\Gamma_1$ ,  $\Gamma_2$  and  $d_2$  were performed at  $Q^2$  well above  $1 \text{ GeV}^2$  where the higher-twist contributions are small compared to the precision of the experiments. However, a good precision test of OPE requires precision data of  $\Gamma_1^n$  starting from  $Q^2$  of about  $0.5 \text{ GeV}^2$  where multiparton interactions are important. From  $Q^2 = 0$  to perhaps  $Q^2 = 0.2 \text{ GeV}^2$ , the moments predicted by the sum rules (e.g. spin polarizabilities etc...) can be calculated in chiral perturbation theory ( $\chi$ PT) [10, 12] and can be tested against experiments. We do not expect OPE or  $\chi$ PT to be valid in the complete range of  $Q^2$ ; however, with time, lattice QCD may bridge the gap between these two limits.

Finally, the  $g_2$  structure function itself is predicted to obey the Burkhardt-Cottingham (BC) sum rule

$$\Gamma_2(Q^2) = \int_0^1 g_2(x, Q^2) dx = 0 \quad (5)$$

which was derived from the dispersion relation and the asymptotic behavior of the corresponding Compton amplitude [20]. This sum rule is also expected to be valid at all  $Q^2$  and does not follow from the OPE. It is a super-convergence relation based on Regge asymptotics as discussed in the review paper by Jaffe [21]. Many scenarios which could invalidate this sum rule have been discussed in the literature [23, 24, 25]. However, this sum rule was confirmed in perturbative QCD at order  $\alpha_s$  with a  $g_2(x, Q^2)$  structure function for a quark target [27]. Surprisingly the first precision measurement of  $g_2$  at SLAC [26] at  $Q^2 = 5 \text{ GeV}^2$  but within a limited range of  $x$  has revealed a violation of this sum rule on the proton at the level of three standard deviations. In contrast, the neutron sum rule is poorly measured but consistent with zero at the one standard deviation.

In this paper, we present measurements of the spin structure functions  $g_1$  and  $g_2$  of  ${}^3\text{He}$  and the determination of  $\Gamma_1^n(Q^2)$ ,  $\Gamma_2^n(Q^2)$  and  $d_2^n(Q^2)$  for the neutron below  $Q^2 = 1 \text{ GeV}^2$ . The data on  $\Gamma_1^n(Q^2)$  and  $d_2^n(Q^2)$  provide a test of the latest results in  $\chi\text{PT}$  and permit a better extraction of  $f_2$ . The data on  $\Gamma_2^n(Q^2)$  allows us to make a more precise test of the neutron BC sum rule at  $Q^2 < 1 \text{ GeV}^2$ .

The features of JLab experiment E94-010, from which these results are derived, were discussed in a previous determination of  $\sigma_{TT'}$ , the transverse-transverse virtual photoabsorption cross section [29]. We measured the inclusive scattering of longitudinally polarized electrons from a polarized  ${}^3\text{He}$  target in Hall A at the Thomas Jefferson National Accelerator Facility (JLab). Data were collected at six incident beam energies: 5.058, 4.239, 3.382, 2.581, 1.718, and 0.862 GeV, all at a nominal scattering angle of  $15.5^\circ$ . The measurements covered values of the invariant mass  $W$  from the quasielastic peak (not discussed in this paper), through the resonance region and continuum. Data were taken for both longitudinal and transverse target polarization orientations. Both spin asymmetries and absolute cross sections were measured. More details can be found in [30].

In the Born approximation  $g_1(x, Q^2)$  and  $g_2(x, Q^2)$  are evaluated by combining data taken with opposite electron beam helicity and parallel or perpendicular target spin with respect to the beam direction.

$$g_1 = \frac{MQ^2\nu}{4\alpha_e^2} \frac{E}{E' E + E'} \left[ \Delta\sigma_{\parallel} + \tan(\theta/2)\Delta\sigma_{\perp} \right] \quad (6)$$

$$g_2 = \frac{MQ^2\nu^2}{4\alpha_e^2} \frac{1}{2E'(E + E')} \left[ -\Delta\sigma_{\parallel} + \frac{E + E' \cos\theta}{E' \sin\theta} \Delta\sigma_{\perp} \right],$$

where  $\Delta\sigma_{\parallel(\perp)} = d^2\sigma^{\downarrow\uparrow(\Rightarrow)}/d\Omega dE' - d^2\sigma^{\uparrow\uparrow(\Rightarrow)}/d\Omega dE'$  is the difference of cross sections for the case in which the target spin is aligned parallel (left-perpendicular) to the beam momentum. Here  $\alpha_e$  is the electromagnetic coupling constant,  $\theta$  is the scattering angle,  $M$  is the nucleon mass,  $\nu$  is the transferred energy and  $E$  and  $E'$  are the initial and final energies of the incident and scattered electron respectively.

The results of  $g_1$  (circles) and  $g_2$  (squares) for  ${}^3\text{He}$  are shown in Fig. 1 as a function of  $x$  for six values of  $Q^2$  in the range  $0.1 \text{ GeV}^2 \leq Q^2 \leq 0.9 \text{ GeV}^2$ . These structure functions were evaluated at constant  $Q^2$  from those measured at fixed incident beam energies and angle by interpolation (filled symbols), and for a few points (open symbols), extrapolation. The error bars represent the uncertainty due to statistics only, and the grey bands indicate the uncertainty due to systematic errors. The systematic errors result from relative uncertainties of about 5% in the absolute cross sections, 4% in the target polarization, 4% in the beam polarization, and 20% in the radiative corrections at every but the lowest incident beam

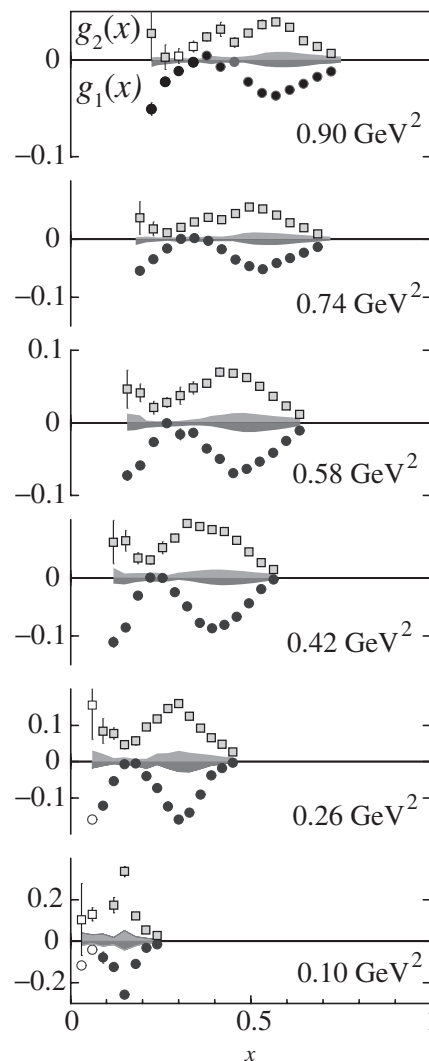


FIG. 1:  $g_1$  (dark filled circles) and  $g_2$  (grey filled squares) of  ${}^3\text{He}$  are plotted as a function of the Bjorken variable  $x$  for six values of  $Q^2$ . The points shown with filled (open) circles or squares were determined by interpolation (extrapolation).

energy where it is 40%. They also include a contribution from interpolation and extrapolation.

We notice a peak in  $g_1$  and  $g_2$  due to the  $\Delta_{1232}$  resonance, which decreases in magnitude with increasing  $Q^2$ . In the vicinity of that resonance  $g_1$  and  $g_2$  are of almost equal amplitude and opposite sign. This is consistent with the fact that the  $\Delta(1232)$  is an M1 resonance, leading us to expect  $\sigma_{LT'} \propto (g_1 + g_2)$ [34] to be highly suppressed. We note also that in a region dominated by the coherent behavior of quarks and gluons (constituent quarks instead of current quarks) the Wandzura-Wilczek relation derived in DIS still holds, perhaps pointing to the role of quark-hadron duality in  $g_1$ .

The integral  $\bar{\Gamma}_1(Q^2)$  for  ${}^3\text{He}$  was computed for each

value of  $Q^2$  using limits of integration extending from the nucleon pion threshold to a value of  $x$  corresponding to  $W = 2.0$  GeV. To extract  $\bar{\Gamma}_1^n(Q^2)$  we followed the prescription suggested by Ciofi degli Atti and Scopetta in [31], where it is found, within the Impulse Approximation, that nuclear effects are quite significant when extracting the spin structure functions, but they reduce to at most 10 % in the extraction of  $\bar{\Gamma}_1^n(Q^2)$ .

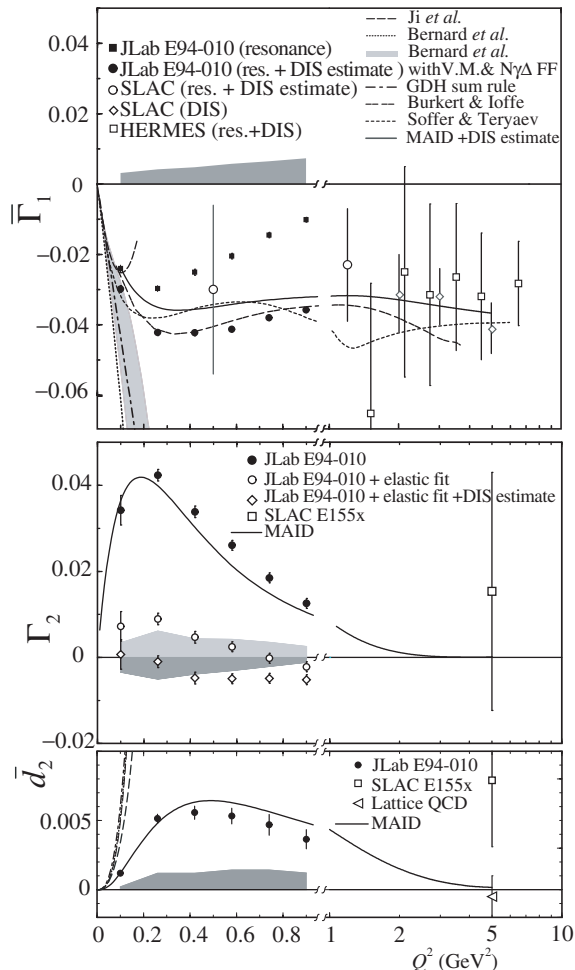


FIG. 2: Results of  $\bar{\Gamma}_1^n$  (top panel),  $\Gamma_2^n$  (middle panel),  $\bar{d}_2^n$  (bottom panels) along with the world data from DIS and theoretical predictions (see text).

The measured values of  $\bar{\Gamma}_1^n(Q^2)$  (solid squares) are shown in Fig. 2 (top panel) at six values of  $Q^2$  along with the world data (open symbols) from SLAC [35] and Hermes [36]. To obtain the total result of  $\bar{\Gamma}_1^n(Q^2)$  (solid circles) an estimated strength in the DIS range  $4 \text{ GeV}^2 < W^2 < 1000 \text{ GeV}^2$  using the parametrization [32, 33] was added to the data obtained in the measured region (solid squares). The size of each symbol indicates the statistical uncertainty while the systematic uncertainties are illustrated with the dark grey band

along the horizontal axis and include the uncertainty of the DIS contribution. We point out that at  $Q^2 > 1 \text{ GeV}^2$  the elastic contribution is negligible and therefore  $\bar{\Gamma}(Q^2) = \Gamma(Q^2)$ .

At low  $Q^2$  we show several  $\chi$ PT calculations; by Bernard *et al.* [11] without vector mesons (dotted line), by Bernard *et al.* [12] including vector mesons and  $\Delta$  degrees of freedom (grey band) and by Ji *et al.* [8] using the HB $\chi$ PT (dashed line). In the calculation of Bernard *et al.* [12] the grey band shows a range of results due to the uncertainty in the  $N\gamma\Delta$  form factor. The latter calculation overlaps with a data point at  $Q^2 = 0.1 \text{ GeV}^2$ . The GDH prediction is the slope depicted by the dot-dashed line at low  $Q^2$ .

At moderate and large  $Q^2$  we show the MAID calculation [34] (used to evaluate the resonance contribution) combined with the DIS estimate from Bianchi and Thomas [32] (solid line). The other calculations shown are by Soffer and Terayev [37] (short-dashed line) and by Burkert and Ioffe [38] (double-dashed line).

While the MAID and Soffer and Terayev calculations are disfavoured, the result from the Burkert and Ioffe calculation agrees well with the data. More importantly, our data above  $Q^2 = 0.5 \text{ GeV}^2$  combined with the world data and future planned measurements [40, 41] in the range  $1 \text{ GeV}^2 < Q^2 < 5 \text{ GeV}^2$  will permit, in the framework of QCD and with better experimental constraints, to repeat the extraction of  $f_2(Q^2)$  higher-twist matrix element performed by Ji and Melnitchouk.

We plot in Fig. 2 (middle panel)  $\Gamma_2^n$  in the measured region (solid circles) and after adding the elastic contribution (open circles) evaluated using the Mergell *et al.* [42] parameterization of  $G_M^n$  and  $G_E^n$ . The open diamonds correspond to the results obtained after adding to the open circles an estimated DIS contribution assuming  $g_2 = g_2^{WW}$  using the same method as described in [26]. Nuclear corrections were performed following a procedure similar to that used in extracting  $\bar{\Gamma}_1^n$  including  $Q^2$  dependent effects [43]. The solid line is the resonance contribution evaluated using MAID. The positive light grey band corresponds to the total experimental systematic errors. The negative dark band is our best estimate of the systematic error for the low  $x$  extrapolation.

Our neutron results (open diamonds) are consistent with the BC sum rule to within 1.7 standard deviations over the measured  $Q^2$  range. The SLAC E155x collaboration [26] previously reported a neutron result at high  $Q^2$  (open square), where the elastic contribution is negligible, consistent with zero but with a rather large error bar. On the other hand, they reported a proton result which deviates from the BC sum rule by 2.8 standard deviations. Their quoted error bar in this case is 3 times smaller than that of the neutron result but still large.

In Fig. 2 (bottom panel),  $\bar{d}_2(Q^2) = d_2(Q^2) - d_2^{\text{elastic}}(Q^2)$  is shown at several values of  $Q^2$ . The results of this experiment are the solid circles. The grey band

represents their corresponding systematic uncertainty. The SLAC E155x [26] neutron result (open square) is also shown. The solid line is the MAID calculation containing only the resonance contribution. At low  $Q^2$  the HB $\chi$ PT calculation[28] (dashed line) and the covariant  $\chi$ PT (dotted line) are shown. The two latter calculations overlap in the  $Q^2$  region shown. Furthermore, calculations of the covariant  $\chi$ PT with the vector mesons contribution (dot-dashed line) and the  $\Delta$  degrees of freedom (long dashed line) are reported [12] but are too close to the former  $\chi$ PT curves to be clearly seen at this scale.

The lattice prediction [19] at  $Q^2 = 5 \text{ GeV}^2$  for the neutron  $d_2$  matrix element is negative but close to zero. We note that all models (not shown at this scale) predict a negative or zero value at large  $Q^2$ . At moderate  $Q^2$  our data show a positive  $\bar{d}_2^n$  and indicate a slow decrease with  $Q^2$ .

In conclusion, we have made the first measurement of  $\Gamma_1^n(Q^2)$ ,  $\Gamma_2^n(Q^2)$  and  $d_2^n(Q^2)$  of the neutron from a  $Q^2$  regime where a twist expansion analysis is appropriate to a regime where  $\chi$ PT can be tested. The BC sum rule for the neutron is verified within errors in the intermediate range of  $Q^2$  due to a cancellation between the resonance and the elastic contributions. Our  $\bar{d}_2^n$  results suggest a positive contribution of the resonance region up to  $Q^2 = 1 \text{ GeV}^2$  of a size comparable to the SLAC E155x result. With time we expect our data, combined with future measurements to provide a challenging test of increasingly precise lattice QCD predictions.

This work was supported by the U.S. Department of Energy (DOE), the U.S. National Science Foundation, the European INTAS Foundation, and the French CEA, CNRS, and Conseil Régional d'Auvergne. The South-eastern Universities Research Association (SURA) operates the Thomas Jefferson National Accelerator Facility for the DOE under contract DE-AC05-84ER40150.

- 
- [1] For recent reviews, see E. W. Hughes and R. Voss, *Ann. Rev. Nucl. Part. Sci.* **49**, 303 (1999) and B. W. Filippone and X. Ji, *Adv. in Nucl. Phys.* **26**, 1 (2001).
- [2] J. D. Bjorken, *Phys. Rev.* **148**, 1467 (1966); *Phys. Rev. D* **1**, 1376 (1970).
- [3] J. Ellis and R.L. Jaffe, *Phys. Rev. D* **9**, 1444 (1974); *D* **10**, 1669 (1974).
- [4] J. Kodaira, S. Matsuda, K Sasaki and T. Uematsu, *Nucl. Phys.* **B159**, 99 (1979).
- [5] J. Kodaira, *Nucl. Phys.* **B165**, 129 (1980).
- [6] S. A. Larin and J. A. M. Vermaseren, *Phys. Lett. B* **259**, 345 (1991) and references therein; S. A. Larin, *Phys. Lett. B* **334**, 192 (1994).
- [7] E.V. Shuryak and A.I. Vainshtein, *Nucl. Phys.* **201**, 141 (1982).
- [8] X. Ji and J. Osborne, *J. of Phys. G* **27**, 127 (2001).
- [9] S.B. Gerasimov, *Sov. J. Nucl. Phys.* **2**, 598 (1965); S.D. Drell and A.C. Hearn, *Phys. Rev. Lett.* **16**, 908 (1966).
- [10] X. Ji, C. Kao, and J. Osborne, *Phys. Lett. B* **472**, 1 (2000).
- [11] V. Bernard, T. Hemmert and Ulf-G. Meissner, *Phys. Lett. B* **545**, 105 (2002).
- [12] V. Bernard, T. Hemmert and Ulf-G. Meissner, *Phys. Rev. D* **67**, 076008 (2003).
- [13] X. Ji, *Nucl. Phys.* **B402** 217 (1993).
- [14] X. Ji and P. Unrau, *Phys. Lett. B* **333**, 228 (1994).
- [15] F. E. Close and R. G. Roberts, *Phys. Lett. B* **336**, 257 (1994).
- [16] X. Ji and W. Melnitchouk, *Phys. Rev. D* **56**, 1 (1997).
- [17] E. Stein, *et al.*, *Phys. Lett. B* **353**, 107 (1995).
- [18] X. Ji, in *Proceeding of the Workshop on Deep Inelastic scattering and QCD*, Editors: JF. Laporte et Y. Sirois Paris, France, 24-28 April, 1995 (ISBN 2-7302-0341-4).
- [19] Göckeler *et al.*, *Phys. Rev. D* **63**, 074506 (2001).
- [20] H. Burkhardt and W. N. Cottingham, *Ann. Phys.* **56**, 453 (1970).
- [21] R. Jaffe, *Comments Nucl. Part. Phys.* **19** (1990) 239.
- [22] S. Wandzura and F. Wilczek, *Phys. Lett. B* **72**, 195 (1977).
- [23] I. P. Ivanov *et al.*, *Phys. Rep.* **320**, 175 (1999).
- [24] M. Anselmino, A. Efremov and E. Leader, *Phys. Rep.* **261**, 1 (1995).
- [25] R. Jaffe and X. Ji, *Phys. Rev. D* **43**, 724 (1991).
- [26] SLAC E155x: P. L. Anthony *et al.*, *Phys. Lett. B* **553**, 18 (2003).
- [27] G. Altarelli, B. Lampe, P. Nason and G. Ridolfi, *Phys. Lett. B* **334**, 187 (1994).
- [28] C. W. Kao, T. Spitzenberg and M. Vanderhaeghen, *Phys. Rev. D* **67**, 016001 (2003).
- [29] M. Amarian *et al.*, *Phys. Rev. Lett.* **89**, 242301 (2002).
- [30] See <http://www.jlab.org/e94010/> for details and theses.
- [31] C. Ciofi degli Atti and S. Scopetta, *Phys. Lett. B* **404**, 223 (1997).
- [32] N. Bianchi and E. Thomas, *Phys. Lett. B* **450**, 439 (1999), *Nucl. Phys. (Proc. Suppl.)* **B 82**, 256 (2000); S.D. Bass and M.M. Brisudova, *Eur. Phys. J. A* **4**, 251 (1999).
- [33] S. D. Bass and A. De Roeck, *Eur. Phys. J. C* **18**, 531 (2001).
- [34] D. Drechsel, S. Kamalov and L. Tiator, *Phys. Rev. D* **63**, 114010 (2001).
- [35] SLAC E142: P. L. Anthony *et al.*, *Phys. Rev. Lett.* **71**, 959 (1993); *Phys. Rev. D* **54**, 6620 (1996); SLAC E143: K. Abe, *et al.*, *Phys. Lett. B* **364**, 61 (1995); K. Abe, *et al.*, *Phys. Rev. D* **58**, 112003 (1998); SLAC E154: K. Abe *et al.*, *Phys. Rev. Lett.* **79**, 26 (1997).
- [36] HERMES: A. Airapetian *et al.*, *Eur. Phys. J. C* **26**, 527 (2003).
- [37] J. Soffer and O. V. Teryaev, *Phys. Lett. B* **545**, 323 (2002)
- [38] V. D. Burkert and B. L. Ioffe, *Phys. Lett. B* **296**, 223 (1992).
- [39] V. D. Burkert and Zh. Li, *Phys. Rev. D* **46**, 47 (1993).
- [40] JLab proposal PR 03-107, spokespersons S. Choi, X. Jiang, and Z.-E. Meziani.
- [41] *The Science Driving the 12 GeV Upgrade at CEBAF*, [http://www.jlab.org/div\\_dept/physics\\_division/GeV.html](http://www.jlab.org/div_dept/physics_division/GeV.html).
- [42] P. Mergell, Ulf-G. Meissner and D. Drechsel, *Nucl. Phys. A* **596**, 367 (1996).
- [43] S. A. Kulagin and W. Melnitchouk (in preparation); W. Melnitchouk (private communication).